

Sensor and Simulation Notes
Note 97
28 January 1970

Some Considerations Concerning a Simulator with the
Geometry of a Cylinder Parallel to and Close to a
Ground or Water Surface

Capt Carl E. Baum
Air Force Weapons Laboratory

Abstract

This note considers some of the performance characteristics of a simulator in which a capacitive pulse generator symmetrically drives a long circular cylinder above and parallel to a ground or water surface. This simulator is considered according to its capability for simulating an incident pulse plane wave which has basically one polarity including a non-zero complete time integral. Special cases of series resistive loading and termination to the ground or water surface are considered using a transmission-line model of the structure which applies for sufficiently low frequencies; the pulse waveforms resulting from this model are compared for the early-time results with the more accurate early-time results obtained by considering the pulse generator and the nearby portions of the simulator as a radiating antenna.

CLEARED FOR PUBLIC RELEASE

RL-94-1092, 13 Dec 94

I. Introduction

In simulating the nuclear electromagnetic pulse (EMP) there is a case of interest in which the EMP is very nearly a free space plane wave incident on a ground or water surface where some system of interest is located. The EMP simulator for such a case might take various approaches to simulating such an incident plane wave. One possible approach consists of a radiating electric dipole antenna in which a capacitive pulse generator is switched into what is basically a long cylindrical antenna. If one is sufficiently far away from such a pulsed antenna then the incident fields can locally approximate an incident plane wave as long as one is considering frequencies high enough that the corresponding wavelengths are short compared to the radius of curvature of the incident spherical wave, which is also the distance from the radiating antenna. One can also use asymptotic far field expressions to calculate the fields provided the observer is sufficiently far from the antenna compared to the antenna dimensions. However, in the far field limit such a pulse-radiating dipole in which the voltage is switched onto the antenna and held there for very late times has a significant limitation in that the radiated pulse has no frequency content at zero frequency; equivalently, such a pulse-radiating antenna has a zero complete time integral which also means that the radiated pulse is not unipolar.^{1,2} If one wishes to simulate an incident plane wave with a frequency content which does not significantly roll off down to rather low frequencies then the pulse-radiating electric dipole has a significant low-frequency limitation.

This low-frequency problem can be overcome by supplementing the high-frequency characteristics of a radiating electric dipole with the low-frequency characteristics of some more appropriate simulator structure which is large enough to place low-frequency fields all over the site of interest on a quasi static basis. This structure should be large enough to avoid significant coupling between the system and simulator structure beyond the coupling of a free field to the system. These types of simulators, combining radiating antenna concepts for high frequencies with static concepts for low frequencies (all in one simulator) might be termed hybrid simulators. One such simulator

1. Capt Carl E. Baum, Sensor and Simulation Note 65, Some Limiting Low-Frequency Characteristics of a Pulse-Radiating Antenna, October 1968.

2. Capt Carl E. Baum, Sensor and Simulation Note 69, Design of a Pulse-Radiating Dipole Antenna as Related to High-Frequency and Low-Frequency Limits, January 1969.

has been considered in a previous note³ in which the large structure over the site is made a half toroid which is connected to the ground surface and is a direct continuation of the pulser region from which high frequencies are radiated. For these hybrid types of simulators the pulser region might be various things such as a bicone structure, a distributed source with a bicone electric field distribution, or perhaps an even larger distributed source launching a more planar wave, somewhat directed at the site being tested. One of the general requirements on these hybrid simulators is that the large simulator structure for the distribution of the low-frequency fields does not interfere with the high-frequency performance by introducing unwanted reflections of the high frequencies; this might be achieved by the shape and sparseness of the structure and by the distribution of appropriate impedances around the structure. The toroidal structure (or TORUS) mentioned above is a possible approach to this hybrid simulator design and it has many desirable features. In this note we consider a different hybrid design which has some (but not all) of the desirable features of the toroidal design. It may also have some advantages of operational convenience in certain conditions of difficult simulator deployment.

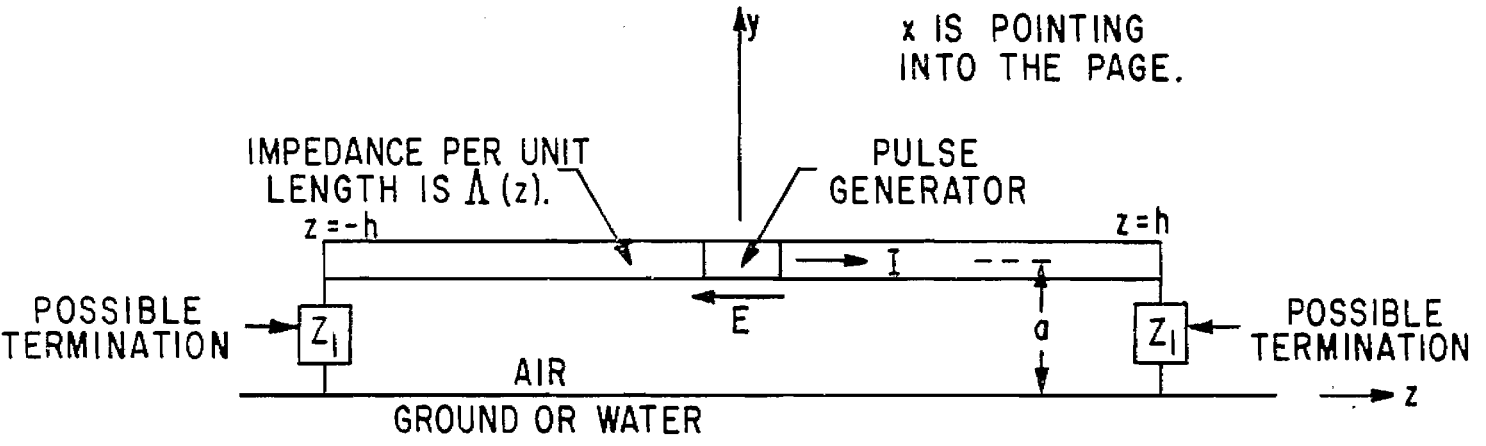
The type of simulator considered in this note uses a capacitive pulse generator switched into a long cylindrical structure. While it can be considered a radiating electric dipole at early times or high frequencies, it is not considered as a radiating antenna but as a quasi static field generator at low frequencies. Basically at low frequencies we have a near field situation; here we are concerned about positions which are close to the simulator compared to the overall simulator dimensions. A further feature of this kind of simulator is that the long cylindrical structure is placed parallel to and near the ground or water surface. Thus the interaction of the simulator structure with the ground or water is part of the simulator performance characteristics.

This topic is of particular interest because some simulators of this general geometry already exist; such as the ones supported by telephone poles and sometimes called "longwires." Furthermore it may be desirable to construct larger versions of this general class of simulators which might rely on other means of support and deployment.

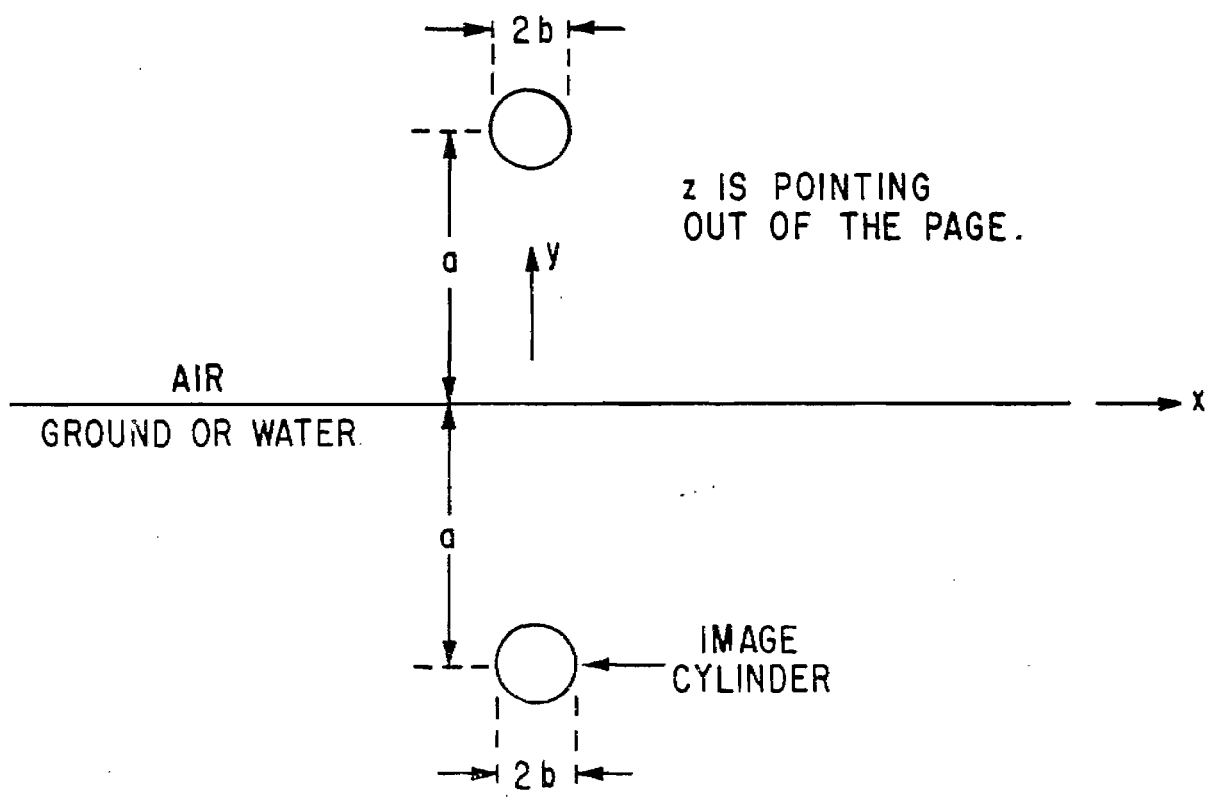
II. Geometry of Simulator

The simulator of interest is sketched in figure 1. It consists of a capacitive pulse generator connected to two cylinders

3. Capt Carl E. Baum, Sensor and Simulation Note 94, Some Considerations Concerning a Simulator with the Geometry of a Half Toroid Joined to a Ground or Water Surface, November 1969.



A. SIDE VIEW



B. END VIEW

FIGURE 1. GEOMETRY OF SIMULATOR

of length h and radius b and aligned as one cylinder on a common axis. These cylinders are aligned parallel to the ground or water surface (assumed flat for the present discussion) and the cylinder axis is at a perpendicular distance a from this surface.

The cylinders are assumed to be loaded with some impedance per unit length $\Lambda(z)$, as yet unspecified, and may (or may not) have a termination impedance Z_1 at each far end of the simulator structure ($z = \pm h$) connecting the simulator structure to the lower medium. The generator is assumed to have a capacitance C_g and charged to an initial voltage V_0 , producing an initial electric field near the generator with polarity as indicated in figure 1. Of course, another alternative is to charge the two ends of the simulator structure to opposite potentials and then discharge them through a switch in place of the full generator. However, the charging time should then be long compared to the longest times of interest to get the desired transient signal. Of course the low-frequency electric fields will be greatly increased and one may be concerned in some cases with nonlinear effects. One might modify $\Lambda(z)$ and/or Z_1 to better accommodate the charging networks involved. If there is only a switch in place of the generator then one can consider the transient problem (changes after the switch closes) by making the generator source impedance zero which corresponds to making C_g infinite.

For coordinates we choose a cartesian (x, y, z) system centered on the ground or water surface with the z axis parallel to the cylinder axis. The x axis is also parallel to this surface and the y axis points up into the air. The cylinder axis is then just $(x, y) = (0, a)$ and the generator is located at $(x, y, z) = (0, a, 0)$. In the next section we also use some coordinates based on the pulser before converting over to the coordinates as above.

As mentioned before we are only considering positions close to the simulator structure compared to h and this will be important for the low-frequency performance of the simulator. Also emphasis is given to positions on the ground or water surface, or better to positions with $|y| \ll a$. The simulator is then considered in its ability to simulate a plane wave incident on the ground or water surface with a particular direction of incidence and polarization by looking at the fields at various positions on the ground or water surface. The lower medium is also assumed to have uniform electrical parameters.

III. Early-Time or High-Frequency Performance

The initial wave radiated from the pulser and the portions of the simulator structure near the generator is not influenced by the presence of the lower medium until the wave reaches this

lower medium. For early times we can consider the pulser and nearby portions of the simulator as a radiating antenna in order to calculate the fields incident on the ground or water surface. In figure 2 we show a spherical coordinate system which we use for this calculation. This spherical coordinate system is centered on the pulser and uses the axis of the simulator structure $(x, y) = (0, a)$ as its axis of symmetry. The spherical coordinates (r, θ, ϕ) are related to the cartesian coordinates (x, y, z) as⁴

$$\begin{aligned} x &= r \sin(\theta) \sin(\phi) \\ y - a &= -r \sin(\theta) \cos(\phi) \end{aligned} \quad (1)$$

$$z = r \cos(\theta)$$

or

$$\begin{aligned} r^2 &= x^2 + (y - a)^2 + z^2 \\ \tan(\theta) &= \frac{1}{z} [x^2 + (y - a)^2]^{1/2} \end{aligned} \quad (2)$$

$$\tan(\phi) = - \frac{x}{y - a}$$

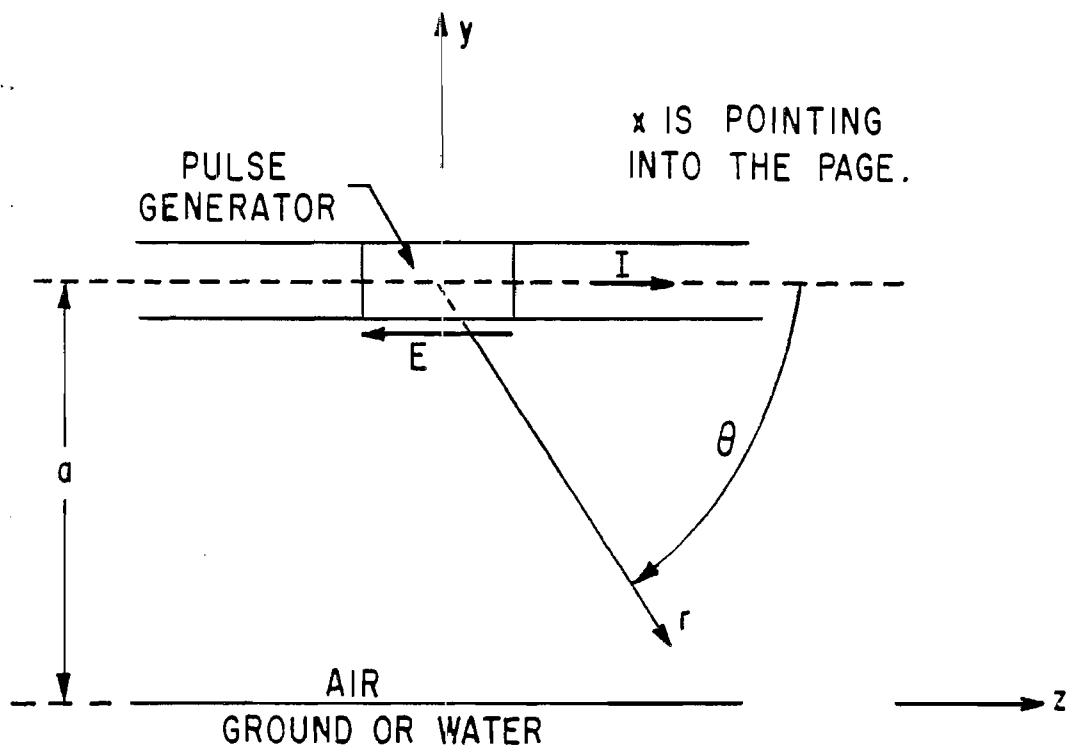
We also have unit vectors for the spherical and cartesian coordinates related as

$$\begin{aligned} \vec{e}_r &= \sin(\theta) \sin(\phi) \vec{e}_x - \sin(\theta) \cos(\phi) \vec{e}_y + \cos(\theta) \vec{e}_z \\ \vec{e}_\theta &= \cos(\theta) \sin(\phi) \vec{e}_x - \cos(\theta) \cos(\phi) \vec{e}_y - \sin(\theta) \vec{e}_z \end{aligned} \quad (3)$$

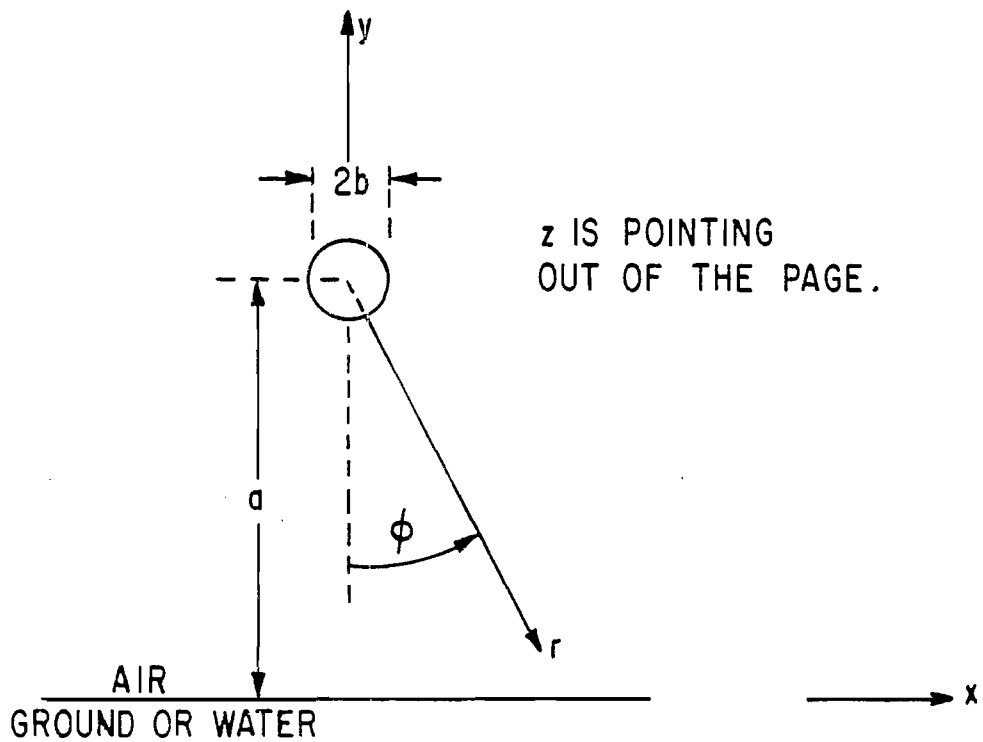
$$\vec{e}_\phi = \cos(\phi) \vec{e}_x + \sin(\phi) \vec{e}_y$$

or

4. All units are rationalized MKSA.



A. SIDE VIEW



B. END VIEW

FIGURE 2. SPHERICAL COORDINATES BASED ON PULSER

$$\begin{aligned}
\vec{e}_x &= \sin(\theta) \sin(\phi) \vec{e}_r + \cos(\theta) \sin(\phi) \vec{e}_\theta + \cos(\phi) \vec{e}_\phi \\
\vec{e}_y &= -\sin(\theta) \cos(\phi) \vec{e}_r - \cos(\theta) \cos(\phi) \vec{e}_\theta + \sin(\phi) \vec{e}_\phi \\
\vec{e}_z &= \cos(\theta) \vec{e}_r - \sin(\theta) \vec{e}_\theta
\end{aligned} \tag{4}$$

Now for the early-time portion of the waveform we assume that the pulse generator is driving a symmetrical bicone (ref. 2) or a distributed source arranged to give a bicone like wave.⁵ Provided the rise time of the wave (zero to peak) is less than the clear time from the ends of the bicone or equivalent distributed source we can simply calculate the peak radiated fields. Let these peak fields at each (r, θ, ϕ) be \vec{E}_1 and \vec{H}_1 and define

$$E_1 \equiv |\vec{E}_1|, \quad H_1 \equiv |\vec{H}_1| \tag{5}$$

Since we are concerned here with a bicone wave we can let

$$\vec{E}_1 \equiv E_1 \vec{e}_\theta, \quad \vec{H}_1 \equiv H_1 \vec{e}_\phi \tag{6}$$

where we have chosen the polarity such that \vec{E}_1 is in the positive θ direction. The generator charge voltage is V_0 and its capacitance is C_0 which is assumed large enough that there is negligible voltage decay during the rise time. The peak field magnitudes are related as

$$E_1 = \frac{V_1}{r \sin(\theta)}, \quad H_1 = \frac{1}{Z_0} \frac{V_1}{r \sin(\theta)} \tag{7}$$

where V_1 is given (from ref. 2) as

$$V_1 = V_0 \left\{ 2 \ln \left[\cot \left(\frac{\theta_0}{2} \right) \right] \right\}^{-1} \tag{8}$$

and where the impedance of free space is

5. Capt Carl E. Baum, Sensor and Simulation Note 84, The Distributed Source for Launching Spherical Waves, May 1969.

$$Z_0 = \sqrt{\frac{\mu_0}{\epsilon_0}} = \frac{E_1}{H_1} \quad (9)$$

The angle θ_0 is a parameter of the bicone or equivalent distributed source and we restrict $\theta_0 < \theta < \pi - \theta_0$ for the above considerations. Note that the bicone clear time is also a function of θ (and also r if one is close to the generator). Typically V_1 might be half of V_0 corresponding to a bicone impedance of roughly 120Ω and a θ_0 of about .7 radians. This parameter (θ_0) can be varied to optimize simulator design. As θ_0 is decreased then the range of θ for which equations 7 apply is increased, but at the same time V_1 is decreased if V_0 is held constant. Since we will get different angles of incidence and polarization by varying θ and ϕ for a given observer (as well as rotating \hat{e}_z with respect to a fixed observer position) then some flexibility in θ is needed in the design of the high-frequency wave launcher. This problem is avoided in the design of the simulator with toroidal geometry because the observer is approximately on the equator of the high-frequency wave launcher.

In reference 3 we discussed the high-frequency and low-frequency characteristics of a plane wave of fixed polarization incident on a uniform semi-infinite conducting dielectric. At low frequencies the only remaining fields are an electric field normal to the surface and a magnetic field parallel to the surface; the electric field is just twice the normal component of the incident electric field and the magnetic field is just twice the horizontal portion of the incident magnetic field, both in magnitude and direction. We wish to see how closely this characteristic is approximated by this simulator.

For this simulator we consider various positions on the ground to get various polarizations and directions of incidence. From a high-frequency viewpoint the direction of incidence is \hat{e}_r and by considering various positions on the x, z plane we find \hat{e}_r can vary in direction to cover 2π steradians except that we do not want \hat{e}_r to be too nearly parallel to the ground or water surface because θ approaches too close to 0 or π and/or the position of observation is too far from the simulator for the present analysis to be valid. Likewise \hat{e}_θ has a similar wide variation over the ground or water surface under the simulator structure. Note that by choosing some x, z combination for the observation position and by appropriately orienting the simulator axis above the surface (i.e. choosing the direction of \hat{e}_z) any direction of incidence and polarization can be chosen subject to the limitation of getting too far from the center of the simulator. In order to orient the simulator with respect to the observation position first choose the direction of incidence; for

a given a this fixes $\sqrt{x^2 + z^2}$ and the direction of the pulse generator from the observation position. Next orient the z axis such that the polarization is fixed as desired.

Another simple way to look at this question is to fix a and then fix \vec{e}_r and \vec{e}_θ (and thus also $\vec{e}_\phi = \vec{e}_r \times \vec{e}_\theta$) in space at the observation position to fix the direction of incidence and polarization respectively. With \vec{e}_r and a we have r and $\sqrt{x^2 + z^2}$. Take \vec{e}_ϕ and project it on the ground or water surface; this projection is normal to the z axis, thus fixing the direction of the z axis if the polarity is included along with \vec{e}_θ .

For later use in comparing the early-time to the low-frequency performance we have the vertical component of the peak incident electric field (in the y direction) as

$$\vec{E}_{1_n} = (\vec{E}_1 \cdot \vec{e}_y) \vec{e}_y = -\cos(\theta) \cos(\phi) E_1 \vec{e}_y \quad (10)$$

The horizontal component of the peak incident magnetic field has only an x component given by

$$\vec{H}_{1_p} = (\vec{H}_1 \cdot \vec{e}_x) \vec{e}_x + (\vec{H}_1 \cdot \vec{e}_z) \vec{e}_z = \cos(\phi) H_1 \vec{e}_x \quad (11)$$

Including the peak field magnitudes from equations 7 gives

$$\vec{E}_{1_n} = -\frac{\cot(\theta) \cos(\phi)}{r} V_1 \vec{e}_y \quad (12)$$

$$\vec{H}_{1_p} = \frac{\csc(\theta) \cos(\phi)}{r} \frac{V_1}{Z_0} \vec{e}_x$$

where r is found from equations 2. This in general is not such a simple dependence as was found for the simulator with a toroidal geometry discussed in reference 3. However, for the special case that on the $y = 0$ plane if also $x = 0$ (making $\phi = 0$) we have

$$\left. \vec{E}_{1_n} \right|_{\substack{x=0 \\ y=0}} = -\frac{\cos(\theta)}{a} V_1 \vec{e}_y$$

$$\vec{H}_{1p} \Big|_{\substack{x=0 \\ y=0}} = \frac{1}{a} \frac{V_1}{Z_0} \vec{e}_x \quad (13)$$

and the magnitudes of the incident fields from equations 7 become

$$E_1 \Big|_{\substack{x=0 \\ y=0}} = \frac{V_1}{a}, \quad H_1 \Big|_{\substack{x=0 \\ y=0}} = \frac{1}{Z_0} \frac{V_1}{a} \quad (14)$$

giving a somewhat simpler dependence. Note that along $(x, y) = (0, 0)$ the incident field magnitudes are constant as long as θ is restricted such that the bicone field distribution in equations 7 applies to the peak incident fields.

Another convenient form for equations 7 is found by using cartesian coordinates as

$$E_1 = V_1 [x^2 + (y - a)^2]^{-1/2} \quad (15)$$

$$H_1 = \frac{V_1}{Z_0} [x^2 + (y - a)^2]^{-1/2}$$

which can be readily applied to the $y = 0$ plane where these peak magnitudes only depend on x . The vertical component of E_1 and horizontal component of H_1 as in equations 12 are likewise

$$\begin{aligned} \vec{E}_{1n} &= \frac{z}{r} (y - a) [x^2 + (y - a)^2]^{-1/2} E_1 \vec{e}_y \\ &= z(y - a) [x^2 + (y - a)^2 + z^2]^{-1/2} [x^2 + (y - a)^2]^{-1} V_1 \vec{e}_y \end{aligned} \quad (16)$$

$$\begin{aligned} \vec{H}_{1p} &= -(y - a) [x^2 + (y - a)^2]^{-1/2} H_1 \vec{e}_x \\ &= -(y - a) [x^2 + (y - a)^2]^{-1} \frac{V_1}{Z_0} \vec{e}_x \end{aligned}$$

For the special case of $y = 0$ (the ground or water surface) these all become

$$\begin{aligned}
 E_1 \Big|_{y=0} &= [x^2 + a^2]^{-1/2} V_1 \\
 H_1 \Big|_{y=0} &= [x^2 + a^2]^{-1/2} \frac{V_1}{Z_0} \\
 \vec{E}_{1n} \Big|_{y=0} &= -za[x^2 + a^2 + z^2]^{-1/2} [x^2 + a^2]^{-1} V_1 \vec{e}_y \\
 \vec{H}_{1p} \Big|_{y=0} &= a[x^2 + a^2]^{-1} \frac{V_1}{Z_0} \vec{e}_x
 \end{aligned} \tag{17}$$

Besides the initial peaks of the fields the rise time characteristics of the pulse are another early-time consideration. These are affected by the design of the pulse generator combined with the bicone or distributed source (or other high-frequency wave-launcher characteristics). The rise-time characteristics are not considered in this note.

IV. Low-Frequency Performance

Now consider the performance of this cylindrical simulator in the low-frequency limit. Suppose we want to simulate an electromagnetic plane wave incident on the ground or water surface and of the form

$$\vec{E}_{inc} = E_2 \left(t - \frac{\vec{r} \cdot \vec{e}_1}{c} \right) \vec{e}_e, \quad \vec{H}_{inc} = \frac{1}{Z_0} E_2 \left(t - \frac{\vec{r} \cdot \vec{e}_1}{c} \right) \vec{e}_h \tag{18}$$

where we assume that $E_2(t) = 0$ for $t < 0$ and that $E_2(t)$ has a positive peak given by

$$E_1 = \max_{0 \leq t \leq \infty} E_2(t) \tag{19}$$

thereby relating the peak of the waveform to the early-time peak discussed in the previous section. Assume that $E_2(t)$ is basically a one-sided pulse with a finite non-zero time integral out to times large compared to times of interest; let this integral be defined as

$$\Phi \equiv \int_0^{\infty} E_2(t) dt \equiv E_1 t_{\text{eff}} = \frac{H_1}{Z_0} t_{\text{eff}} \neq 0 \quad (20)$$

where t_{eff} is a characteristic time for the incident plane wave. The speed of light is

$$c = \frac{1}{\sqrt{\mu_0 \epsilon_0}} \quad (21)$$

The unit vectors in equations 18 give the direction of propagation (\vec{e}_1), the electric field direction (\vec{e}_e), and the magnetic field direction (\vec{e}_h); these are related by

$$\vec{e}_1 \times \vec{e}_e = \vec{e}_h, \quad \vec{e}_e \times \vec{e}_h = \vec{e}_1, \quad \vec{e}_h \times \vec{e}_1 = \vec{e}_e \quad (22)$$

Note that the polarization (\vec{e}_e) and direction of incidence (\vec{e}_1) are assumed time independent.

For the simulator under consideration we take some reference point for an observer on the ground or water surface (the $y = 0$ plane), chosen to give the desired direction of incidence and polarization for the early-time fields as discussed in the previous section. Considering just this reference point we set

$$\vec{e}_1 \equiv \vec{e}_r, \quad \vec{e}_e \equiv \vec{e}_\theta, \quad \vec{e}_h \equiv \vec{e}_\phi \quad (23)$$

Of course as one moves away from this reference point \vec{e}_r , \vec{e}_θ , and \vec{e}_ϕ change in general, changing the early-time direction of incidence and polarization. However, if one only considers small position variations near the reference point the variation of direction of incidence and polarization will also be small.

In simulating the incident plane wave as in equations 18 at the position of the observer on the $y = 0$ plane we now try to make the low-frequency content of the simulator waveform at the observer match what would be produced by an incident plane wave with a direction of incidence and polarization already fixed to match the early-time simulator performance. At low frequencies the resultant field from an incident plane wave at the surface

of a semi-infinite conducting medium has only a normal electric field and a parallel magnetic field which are just twice the values of the field components in the incident wave. Since the complete time integral is the same as the Fourier transform evaluated at zero frequency, we have the complete time integrals of the resultant fields from an incident plane wave (equations 18) as

$$\begin{aligned}
 \int_0^{\infty} \vec{E}_{res} dt &= 2\vec{e}_y \left[\vec{e}_y \cdot \int_0^{\infty} \vec{E}_{inc} dt \right] = 2\phi (\vec{e}_\theta \cdot \vec{e}_y) \vec{e}_y \\
 &= -2\cos(\theta) \cos(\phi) \phi \vec{e}_y \\
 &= 2z(y-a) [x^2 + (y-a)^2 + z^2]^{-1/2} [x^2 + (y-a)^2]^{-1/2} \phi \vec{e}_y
 \end{aligned} \tag{24}$$

$$\begin{aligned}
 \int_0^{\infty} \vec{H}_{res} dt &= 2\vec{e}_x \left[\vec{e}_x \cdot \int_0^{\infty} \vec{H}_{inc} dt \right] + 2\vec{e}_z \left[\vec{e}_z \cdot \int_0^{\infty} \vec{H}_{inc} dt \right] \\
 &= 2 \frac{\phi}{z_0} (\vec{e}_x \cdot \vec{e}_\phi) \vec{e}_x = 2\cos(\phi) \frac{\phi}{z_0} \vec{e}_x \\
 &= -2(y-a) [x^2 + (y-a)^2]^{-1/2} \frac{\phi}{z_0} \vec{e}_x
 \end{aligned}$$

We have used \vec{E}_{res} and \vec{H}_{res} here to denote the desired plane wave results which may have some difference from the simulator results. Note that equations 24 are easily specialized to the ground or water surface ($y = 0$).

Having the low-frequency fields to be simulated we need to compare these to the simulator performance in the low-frequency limit. First we consider the effect of ground or water conductivity in changing the low-frequency performance and then the effect of omitting or including a resistive termination Z_1 (as in figure 1).

A. Effect of Large and Small Ground or Water Conductivities

At low frequencies the electromagnetic field distribution is significantly influenced by the conductivity σ of the ground or

water medium. Consider frequencies with corresponding wavelengths much larger than a so that one can use transmission-line approximations to describe the fields in the simulator for distances much closer to the structure than h and not too near the ends ($z = \pm h$) or middle ($z = 0$) of the simulator. Note that the magnetic field near $z = 0$ can still be estimated this way because the current on the structure at these low frequencies will be continuous through $z = 0$. For a given frequency the fields and currents in the ground are affected by σ in the sense of a skin depth in the lower medium and by the geometry of the simulator, i.e. a cylinder above and parallel to a semi-infinitely conducting half space.

In this note we consider two special limiting cases to shed some light on the low-frequency performance of the simulator. First we consider the case of $\sigma = \infty$ so that $y = 0$ is a perfectly conducting plane. Second we consider σ finite (but non-zero) and let the frequency go to zero. Strictly speaking the second case represents the low-frequency limit since σ is in general finite. However for a lower medium with sufficiently high σ then at frequencies low enough for the current and charge on the structure to have nearly reached their low-frequency asymptotic values the skin depth in the lower medium may still be less than a . For such high σ cases the limit of $\sigma \rightarrow \infty$ is still meaningful, although as $\omega \rightarrow 0$ the finite σ case eventually applies.

Case 1: Large Conductivity for Lower Medium

If we set $\sigma = \infty$ and consider the low-frequency performance of the simulator we can use an image calculation whereby the $y = 0$ plane is a symmetry plane in a transmission line consisting of two cylinders. In another note we have considered the impedance and field distribution for this geometry.⁶ The characteristic impedance of the two wire system is

$$Z_{\infty} = Z_0 f_g \quad (25)$$

where

$$f_g = \frac{1}{\pi} \operatorname{arccosh}\left(\frac{a}{b}\right) = \frac{1}{\pi} \ln \left[\frac{a}{b} + \left(\left(\frac{a}{b}\right)^2 - 1 \right)^{1/2} \right] \quad (26)$$

For large a/b we have, as $a/b \rightarrow \infty$,

⁶. Lt Carl E. Baum, Sensor and Simulation Note 27, Impedances and Field Distributions for Symmetrical Two Wire and Four Wire Transmission Line Simulators, October 1966.

$$\begin{aligned}
f_g &= \frac{1}{\pi} \ln\left(2 \frac{a}{b}\right) + \frac{1}{\pi} \ln\left[\frac{1}{2} + \frac{1}{2}\left(1 - \left(\frac{b}{a}\right)^2\right)^{1/2}\right] \\
&= \frac{1}{\pi} \ln\left(2 \frac{a}{b}\right) + \frac{1}{\pi} \ln\left[1 - \frac{1}{4}\left(\frac{b}{a}\right)^2 + o\left(\left(\frac{b}{a}\right)^4\right)\right] \\
&= \frac{1}{\pi} \ln\left(2 \frac{a}{b}\right) - \frac{1}{4\pi}\left(\frac{b}{a}\right)^2 + o\left(\left(\frac{b}{a}\right)^4\right)
\end{aligned} \tag{27}$$

The characteristic impedance of a single cylinder over the $y = 0$ plane is just $Z_\infty/2$. However for two such transmission lines driven in series by the pulse generator the factor of two re-enters making Z_∞ the appropriate characteristic impedance for the simulator geometry. Note that Z_∞ does not include any series impedance $\Lambda(z)$ in the cylindrical conductors; this will be added later. $\Lambda(z)$ is assumed even in z so that the simulator is symmetric about $z = 0$ and the two transmission lines ($z > 0$ and $z < 0$) are identical and the series combination can be considered as a single transmission line for calculational purposes.

Here we are concerned with relating the electric and magnetic fields to the voltage and current on the simulator structure. Again from reference 6 we have the electric field on the z axis with only a y component as

$$E_y \Big|_{\substack{x=0 \\ y=0}} = - \frac{V}{2(a-b)} f_e \tag{28}$$

where

$$f_e = \frac{2}{\operatorname{arccosh}\left(\frac{a}{b}\right)} \left[\frac{\frac{a}{b} - 1}{\frac{a}{b} + 1} \right]^{1/2} = \frac{2}{\pi f_g} \left[\frac{\frac{a}{b} - 1}{\frac{a}{b} + 1} \right]^{1/2} \tag{29}$$

and where V is a function of z and is the potential on the structure at z minus the potential at $-z$. $V/2$ is defined as the potential difference between the simulator structure and the $y = 0$ plane (perfectly conducting) at fixed z . Thus taking the two halves of the simulator in series to give an effective transmission line driven by the pulser makes $V(z)$ the voltage along the transmission line where we consider z positive for later transmission-line calculations of voltages and currents.

In another form we have

$$E_y \Big|_{\substack{x=0 \\ y=0}} = - \frac{V}{\pi f_g} [a^2 - b^2]^{-1/2} \quad (30)$$

For other positions on a plane of constant z we have (from reference 6)

$$E_y = - \frac{V}{\pi f_g} [a^2 - b^2]^{-1/2} \frac{a}{2} \left\{ \frac{a+y}{x^2 + (a+y)^2} + \frac{a-y}{x^2 + (a-y)^2} \right\} \quad (31)$$

$$E_x = - \frac{V}{\pi f_g} [a^2 - b^2]^{-1/2} \frac{a}{2} \left\{ \frac{x}{x^2 + (a+y)^2} - \frac{x}{x^2 + (a-y)^2} \right\}$$

On the $y = 0$ plane these become

$$E_y = - \frac{V}{\pi f_g} [a^2 - b^2]^{-1/2} \frac{a^2}{x^2 + a^2} \quad (32)$$

$$E_x = 0$$

Compare this distribution of E_y on the $y = 0$ plane with that desired from an incident plane wave in equations 24 (chosen to match the initial fields to reach the observer). Note that these distributions are not the same on the $y = 0$ plane. As a special case one might look at $z = 0$ so that E_y for an incident plane wave is zero. At $z = 0$ the transmission-line approximation for E_y does not apply and E_y is zero for all time because of symmetry in z .

The magnetic field in our transmission-line model for the simulator on the z axis with only an x component is given by

$$\begin{aligned} H_x \Big|_{\substack{x=0 \\ y=0}} &= \frac{I}{2(a-b)} f_g f_e \\ &= \frac{I}{\pi} [a^2 - b^2]^{-1/2} \end{aligned} \quad (33)$$

where I is the current in the cylindrical structure as shown in figure 1; I is a function of z. For other positions on a plane of constant z we have

$$H_x = \frac{I}{\pi} [a^2 - b^2]^{-1/2} \frac{a}{2} \left\{ \frac{a+y}{x^2 + (a+y)^2} + \frac{a-y}{x^2 + (a-y)^2} \right\}$$

$$H_y = \frac{I}{\pi} [a^2 - b^2]^{-1/2} \frac{a}{2} \left\{ \frac{-x}{x^2 + (a+y)^2} + \frac{x}{x^2 + (a-y)^2} \right\}$$
(34)

On the $y = 0$ plane these become

$$H_x = \frac{I}{\pi} [a^2 - b^2]^{-1/2} \frac{a^2}{x^2 + a^2}$$

$$H_y = 0$$
(35)

Comparing this distribution with that in equation 24 on the $y = 0$ plane note that the x dependence is the same. Also if I at low frequencies is not a function of z there is the same z dependence. Of course there is a restriction on the early-time results used to define an incident plane wave that $\theta_0 < \theta < \pi - \theta_0$ (or perhaps even more restricted) so that the form of the incident fields used at early times is valid.

Case 2: Small Conductivity for Lower Medium

If the conductivity σ of the lower medium is low enough that for low frequencies of interest the skin depth is large compared to a then we have a second limiting case. As long as the electric field for $y < 0$ is negligible compared to that for $y > 0$ we can use the results of equations 31 to describe the electric field distribution for $y > 0$ in the transmission-line approximation. This requires that the ground conductivity not be so low that the currents in the ground are associated with a significant electric field. Roughly this requires that the effective impedances associated with the lower medium be small compared to both Z_∞ and the termination impedance.

On the other hand the magnetic field distribution at low frequencies is significantly changed by a low ground or water conductivity. If the skin depth is large compared to a then the magnetic field near the simulator (distances comparable to a or less) is just given on a plane of constant z by

$$\vec{H}' = \frac{I}{2\pi r \sin(\theta)} \vec{e}_\phi = \frac{I}{2\pi} [x^2 + (a - y)^2]^{-1/2} \vec{e}_\phi \quad (36)$$

or

$$H'_x = \frac{I}{2\pi} \frac{a - y}{x^2 + (a - y)^2} \quad (37)$$

$$H'_y = \frac{I}{2\pi} \frac{x}{x^2 + (a - y)^2}$$

This is just the magnetic field for a current at $(x, y) = (0, a)$, the current in the ground being on the average far away from the observer compared to a . On the $y = 0$ plane we have

$$H'_x = \frac{I}{2\pi} \frac{a}{x^2 + a^2} \quad (38)$$

$$H'_y = \frac{I}{2\pi} \frac{x}{x^2 + a^2}$$

Note that we use primes for the fields for this small σ case to differentiate the results from the large σ case.

Comparing equations 38 and 35 note for $b \ll a$ that H'_x is just half of H_x (for the same I) on the $y = 0$ plane. An H'_y is also introduced whereas $H_y = 0$ on the $y = 0$ plane. Note that these two cases of large and small σ are limiting cases of what happens at low frequencies of interest. In practical situations one may often be in a transition region between these two cases for low frequencies of interest.

B. Low-Frequency Performance for Unterminated Simulator

Now let $Z_1 = \infty$ where the termination impedance Z_1 is at two positions $z = \pm h$ as shown in figure 1. With the generator assumed to be a capacitance C_g switched onto the simulator at $t = 0$, and with no impedances to remove charge from the antenna in late times of interest then the simulator capacitance C_a dominates the problem. The simulator capacitance per unit length is

$$C' = \frac{\epsilon_0}{F_g} \quad (39)$$

where ϵ_0 is the permittivity of free space and the total simulator capacitance is just

$$C_a = hC' = \frac{\epsilon_0 h}{f_g} = \pi \epsilon_0 h \left\{ \ln \left[\frac{a}{b} + \left(\left(\frac{a}{b} \right)^2 - 1 \right)^{1/2} \right] \right\}^{-1} \quad (40)$$

where f_g is found in equations 26 and 27. Note that C' is defined per unit length of the two ends of the simulator ($z > 0$ and $z < 0$) considered in series as a single transmission line; this C' is consistent with Z_∞ in equation 25.

With $Z_1 = \infty$ then in the low-frequency limit there is no current and no electric field in the lower medium while the simulator is charged and there is electric field above the ground. Thus C_a should be accurately represented by equation 40 in the limit as $a/h \rightarrow 0$. Note that fringing electric fields near $z = 0$ and $z = \pm h$ have been neglected in calculating this capacitance; these fringing fields will slightly increase C_a .

Define a capacitance parameter as

$$\alpha \equiv 1 + \frac{C_a}{C_g} \quad (41)$$

With V_0 as the initial volts on the generator the volts on the transmission line in the late time limit are

$$\lim_{t \rightarrow \infty} V \equiv V_\infty = \frac{V_0}{\alpha} \quad (42)$$

where z has been taken positive for V and where the result comes from charge conservation. Note that V_∞ is not a function of z . The late-time voltage of the simulator with respect to the $y = 0$ plane is $+V_\infty/2$ for $z > 0$ and $-V_\infty/2$ for $z < 0$. Substituting V_∞ for V in equations 32 gives the late-time electric field distribution on the $y = 0$ plane as

$$E_y = - \frac{|z|}{z} \frac{V_\infty}{\pi f_g} [a^2 - b^2]^{-1/2} \frac{a^2}{x^2 + a^2} \quad (43)$$

$$E_x = 0$$

where $|z|/z$ accounts for the change in electric field polarity at $z = 0$. In equations 24 we give a characteristic of the electric field waveform for a desired incident plane wave in which the complete time integral of the waveform is finite and non-zero. The electric field waveform associated with this un-terminated and non-decaying simulator has an infinite complete time integral (in the limiting case) implying a much larger low-frequency content for sufficiently small frequency. Depending on the magnitude of α the late-time electric field could be comparable to the desired transient electric field and for high-level simulation one might be concerned with nonlinear effects.

The initial charge on the generator is

$$Q_0 = V_0 C_g \quad (44)$$

The late-time charge on the simulator is

$$Q_\infty = V_\infty C_a = \frac{V_0}{\alpha} C_a = \frac{C_a C_g}{C_a + C_g} V_0 \quad (45)$$

where this is the charge for $z > 0$; for $z < 0$ the charge is $-Q_\infty$. This charge is the complete time integral of the current leaving the pulser. Now Q_∞ is uniformly distributed over $0 < z < h$, neglecting fringe electric fields near $z = 0$ and $z = h$. Thus the complete time integral of the current is

$$\int_0^\infty I dt = \left[1 - \frac{|z|}{h}\right] Q_\infty \quad (46)$$

where I is taken positive in the $+z$ direction; $|z|$ is used to make this result apply for $-h < z < h$. Note that I is continuous through $z = 0$ so that this can be used for the magnetic field near $z = 0$.

Consider as a first case that the lower medium conductivity is arbitrarily large so that we set $\sigma = \infty$. Equations 34 relate the current and magnetic field in the transmission-line approximation; equations 35 give the simpler results for the magnetic field on the $y = 0$ plane. The low-frequency content of the magnetic field is just the complete time integral of the time domain waveform. From equations 35 and 46 we then have on the $y = 0$ plane

$$\int_0^{\infty} H_x dt = \frac{1}{\pi} [a^2 - b^2]^{-1/2} \frac{a^2}{x^2 + a^2} \left[1 - \frac{|z|}{h} \right] Q_{\infty} \quad (47)$$

$$\int_0^{\infty} H_y dt = 0$$

Now to match the desired complete time integral to simulate an incident plane wave as in equations 24 we have on the $y = 0$ plane the requirement

$$Q_{\infty} = \frac{2\pi}{a} [a^2 - b^2]^{1/2} [x^2 + a^2]^{1/2} \left[1 - \frac{|z|}{h} \right]^{-1} \frac{\phi}{z_0} \quad (48)$$

showing that for given ϕ , a , and b then Q_{∞} (and thus Q_0) must be changed as the simulator is moved to make the observer be at a certain (x, z) . Equation 20 relates the waveform peak to a characteristic time t_{eff} for the desired plane wave. Equations 17 give this peak on the $y = 0$ plane as a function of x and z . These give for equation 48

$$Q_{\infty} = \frac{2\pi}{a} [a^2 - b^2]^{1/2} \left[1 - \frac{|z|}{h} \right]^{-1} \frac{V_1}{z_0} t_{\text{eff}} \quad (49)$$

Solving for t_{eff} and using equation 45 for Q_{∞} gives

$$t_{\text{eff}} = \frac{a}{2\pi} [a^2 - b^2]^{-1/2} \left[1 - \frac{|z|}{h} \right] z_0 \frac{V_0}{V_1} \frac{C_a C_g}{C_a + C_g} \quad (50)$$

For fixed a , b , h , C_g , and V_0/V_1 (equation 8) then t_{eff} is only a function of z , and if we restrict $|z| \ll h$ (i.e. keep near the middle of the simulator) then the dependence on z is small. Note that the horizontal component of the magnetic field is in the x direction at both early times and low frequencies, allowing one to match the desired characteristics of H_{inc} in both limits.

As a second case let the lower medium have finite σ , small enough for low frequencies of interest that the skin depth in the lower medium is large compared to a and the results of equations 36 through 38 apply. Note that for this case as long as the electric field in the lower medium can be neglected the results for the electric field are the same as for the $\sigma = \infty$ case

in equations 42 and 43. For the magnetic field on the $y = 0$ plane substitute from equations 38 into equation 46 to give (using primes for this low conductivity case)

$$\int_0^{\infty} H'_x dt = \frac{1}{2\pi} \frac{a}{x^2 + a^2} \left[1 - \frac{|z|}{h} \right] Q_{\infty} \quad (51)$$

$$\int_0^{\infty} H'_y dt = \frac{1}{2\pi} \frac{x}{x^2 + a^2} \left[1 - \frac{|z|}{h} \right] Q_{\infty}$$

Note for $b \ll a$ that the complete time integral of H'_x is just one half the result for H_x in equations 47 and that H'_y has a non-zero complete time integral for $x \neq 0$, $|z| < h$. If we consider $x = 0$ then the complete time integral of H'_y is zero. In order to match the desired complete time integral as in equations 24 let us just consider H'_x giving the requirement on the $y = 0$ plane

$$Q_{\infty} = 4\pi [x^2 + a^2]^{1/2} \left[1 - \frac{|z|}{h} \right]^{-1} \frac{\phi}{z_0} \quad (52)$$

In terms of the characteristic time t_{eff} desired for the pulse this result is

$$Q_{\infty} = 4\pi \left[1 - \frac{|z|}{h} \right]^{-1} \frac{V_1}{z_0} t_{\text{eff}} \quad (53)$$

Solving for t_{eff} and substituting for Q_{∞} gives

$$t_{\text{eff}} = \frac{1}{4\pi} \left[1 - \frac{|z|}{h} \right] z_0 \frac{V_0}{V_1} \frac{C_a C_g}{C_a + C_g} \quad (54)$$

This result for finite σ is approximately one half the result in equation 50 for the $\sigma = \infty$ case (for the same voltages and capacitances).

Looking at the results for both large and small σ we observe that it is quite possible to have a non-zero complete time integral of the magnetic field waveform if the capacitive pulse generator discharges into the simulator without letting the charge decay across the generator at late times of interest.

This is in sharp contrast to a pulse-radiating antenna as discussed in references 1 and 2 where we were concerned with the radiated far fields. Here we have a near field problem for low frequencies because the observer is close to the simulator compared to h . This result is further altered by the presence of the lower medium which changes the near field distribution but keeps a non-zero complete time integral for the magnetic field. On the other hand the electric field has a non-zero late time limit implying an infinite complete time integral (or low-frequency content in the limit of zero frequency). In this respect the unterminated simulator gives more than desired at low frequencies. Of course, for large enough times the charge on the simulator will go to zero, if only so that the generator can be recharged. Perhaps these times can be much larger than late times of interest corresponding to frequencies much lower than low frequencies of interest for a simulation test. On the other hand the vastly increased low-frequency electric field may represent a severe overtest or even induce nonlinear effects at high levels in some cases.

C. Low-Frequency Performance for Simulator with a Termination which is Resistive at Low Frequencies

Having considered the case of $Z_1 = \infty$ we go on to the case where Z_1 has a finite resistive value in the low-frequency limit. In this case we have

$$\int_0^{\infty} I dt = Q_0 = V_0 C_g \quad (55)$$

i.e. the total charge on the generator passes through the simulator structure, termination, and lower medium to completely drain the generator in the late-time limit. Define a low-frequency impedance per unit length for the simulator structure as

$$\Lambda_0(z) \equiv \lim_{\omega \rightarrow 0} \Lambda(z) \geq 0 \quad (56)$$

which we also assume to be finite, or at least to have integrable singularities such that

$$R_0 \equiv \int_0^h \Lambda_0(z) dz \quad (57)$$

is finite. Note Λ_0 is assumed non negative so that it is a passive resistance. Then the low-frequency voltage on the simulator, neglecting low-frequency electric fields in the lower medium, is

$$\begin{aligned}
\int_0^{\infty} V dt &= 2 \frac{|z|}{z} \left\{ R_1 + \int_z^h \Lambda(z') dz' \right\} \int_0^{\infty} I dt \\
&= 2 \frac{|z|}{z} \left\{ R_1 + \int_z^h \Lambda(z') dz' \right\} Q_0
\end{aligned} \tag{58}$$

where we have defined

$$R_1 \equiv \lim_{\omega \rightarrow 0} Z_1 \tag{59}$$

and where (as discussed before) $V/2$ is the voltage of the simulator structure with respect to the lower medium. Again the impedance of the lower medium has been assumed small enough that it can be neglected.

Having the low-frequency current and voltage, next consider the low-frequency fields. The low-frequency magnetic field (which is the complete time integral) is considered first for the case of $\sigma = \infty$ so that equations 34 and 35 apply. On the $y = 0$ plane for this high conductivity case we have

$$\int_0^{\infty} H_x dt = \frac{1}{\pi} [a^2 - b^2]^{-1/2} \frac{a^2}{x^2 + a^2} Q_0 \tag{60}$$

$$\int_0^{\infty} H_y dt = 0$$

Matching the desired complete time integral as in equations 24 gives

$$Q_0 = \frac{2\pi}{a} [a^2 - b^2]^{1/2} [x^2 + a^2]^{1/2} \frac{\phi}{Z_0} \tag{61}$$

Equation 20 relates the waveform peak to a characteristic time t_{eff} for the desired plane wave, and equations 17 give this peak on the $y = 0$ plane so that equation 61 becomes

$$Q_0 = \frac{2\pi}{a} [a^2 - b^2]^{1/2} \frac{V_1}{Z_0} t_{\text{eff}} \tag{62}$$

Solving for t_{eff} and substituting for Q_0 gives

$$t_{\text{eff}} = \frac{2}{2\pi} [a^2 - b^2]^{-1/2} z_0 \frac{V_0}{V_1} C_g \quad (63)$$

For fixed a , b , C_g , and V_0/V_1 then t_{eff} is independent of the coordinates on the $y = 0$ plane, provided the earlier restrictions on coordinate variation are met.

On the other hand for the finite σ case for the lower medium equations 36 through 38 apply. For the low-frequency magnetic field on the $y = 0$ plane we have (using primes for this low conductivity case) from equation 38

$$\int_0^{\infty} H'_x dt = \frac{1}{2\pi} \frac{a}{x^2 + a^2} Q_0 \quad (64)$$

$$\int_0^{\infty} H'_y dt = \frac{1}{2\pi} \frac{x}{x^2 + a^2} Q_0$$

Again note that the complete time integral of H'_y is non-zero for this finite σ case. Considering only H'_x in matching the desired complete time integral in equation 24 on the $y = 0$ plane gives

$$Q_0 = 4\pi [x^2 + a^2]^{1/2} \frac{\phi}{z_0} \quad (65)$$

Substituting for ϕ (as before) we have, in terms of the characteristic time t_{eff} ,

$$Q_0 = 4\pi \frac{V_1}{z_0} t_{\text{eff}} \quad (66)$$

Solving for t_{eff} and substituting for Q_0 gives

$$t_{\text{eff}} = \frac{1}{4\pi} z_0 \frac{V_0}{V_1} C_g \quad (67)$$

This result is about one half of the result for the high σ case in equation 63.

Assuming σ is large enough that electric fields for $y < 0$ can be neglected compared to those for $y > 0$ then for both high and low σ cases for low frequencies we can use equations 31, 32, and 58 to find the electric field above the $y = 0$ plane, giving on the $y = 0$ plane

$$\int_0^{\infty} E_Y dt = - \frac{|z|}{z} \frac{1}{\pi f_g} [a^2 - b^2]^{-1/2} \frac{a^2}{x^2 + a^2} \left\{ R_1 + \int_z^h \Lambda(z') dz' \right\} Q_0 \quad (68)$$

$$\int_0^{\infty} E_X dt = 0$$

Matching the desired complete time integral on the $y = 0$ plane from equations 24 gives

$$Q_0 = \frac{\pi f_g}{a} [a^2 - b^2]^{1/2} [x^2 + a^2]^{1/2} [x^2 + a^2 + z^2]^{-1/2} |z| \Phi \cdot \left\{ R_1 + \int_z^h \Lambda(z') dz' \right\}^{-1} \quad (69)$$

Comparing this result to equation 61 for the large σ case and to equation 65 for the small σ case, note the additional dependence on the coordinates in equation 69. However there is also the term involving the integral of $\Lambda(z')$ from z to h ; this term can be used (together with R_1) to make the Q_0 required from electric field considerations approximate the Q_0 required from magnetic field considerations (equation 61 or 65). Note that the electric field result in equation 68 does not apply near $z = 0$ and $z = +h$ as well as a z near which $\Lambda(z)$ is so large as to make the integral of $\Lambda(z')$ change too abruptly.

D. Some Further Comments on Low-Frequency Performance

As one can see there is a fair amount of flexibility in choosing the simulator parameters such as a , b , h , V_0 , V_1 , and C_g as well as the orientation of the simulator with respect to the system under test. Appropriately choosing these parameters one can vary the peak fields, direction of incidence, polarization, and low-frequency field characteristics. The type of termination Z_1 and series impedance per unit length $\Lambda(z)$ can also be varied to change the low-frequency field characteristics for both electric and magnetic fields, including their relationship to each other.

One of the optional ways of operating such a simulator is to replace the pulse generator with a switch, slowly charge the two halves of the simulator structure with respect to each other, and initiate the pulse by closing the switch at $z = 0$. This technique introduces certain features into the simulator. The charging of the simulator structure requires charging through some current paths connected to the simulator. Also Z_1 cannot bleed off charge during the charging period so that Z_1 must have a large magnitude at low frequencies. One might combine Z_1 with the charging system so that with equal and opposite charging at each end the transient representation of Z_1 might be a very large resistance or perhaps a series RC network or some other network which looks like a capacitance for low frequencies. Considering the waveform in the time domain one must have the charging time large compared to all times of interest if the transient pulse is to be considered solely; in the frequency domain this means that frequencies in the charging waveform be lower than all frequencies of interest. Of course these considerations assume linearity in the response of the system under test to the applied waveform. However, if there are significant nonlinear effects which are initiated or coupled to by the slow but large fields in the charging period (particularly electric fields) then this type of charging system does not give as good a simulator as one with the generator at $z = 0$ so that the structure is initially uncharged. Of course there are other deficiencies which are generally associated with any simulator and such slow time or low-frequency problems may be acceptable in some cases.

Note that if a switch is used to switch a charged simulator structure this corresponds to making C_g infinite because transiently the "generator" impedance is a short circuit (except for some inductance and other high-frequency perturbations). In addition there may be other capacitances introduced (say in Z_1) associated with the charging system. These capacitance changes will have to be included in the equations of this section to properly describe the performance of the simulator for low frequencies of interest. Also there are appropriate changes in the polarities so that V_0 represents the applied transient voltage and the resulting fields are the transient fields or changes in the fields after the switch closes.

V. Transmission-Line Model

Having considered the early-time and low-frequency results for this simulator geometry we now consider some approximate results for intermediate frequencies based on a transmission-line model of the simulator. With $b \ll a$ this model should apply for radian frequencies ω small compared to c/a . In the time domain this should apply for pulses with pulse widths large compared to a/c except for early times of the order of a/c and less after the initial signal reaches the observer.

For the transmission-line calculations of this section we only consider the case of infinite conductivity for the lower medium so that we do not have to include an impedance per unit length for the lower medium as part of the equivalent transmission line. Perhaps in future notes the finite ground conductivity could be included, or perhaps even a more complete wave solution for the simulator geometry could be developed.

In figure 3 we show the simulator represented as an equivalent transmission line. Defining

$$\zeta \equiv |z|$$

$$Z_t \equiv 2Z_1 \tag{70}$$

$$Z'(\zeta) \equiv 2\Lambda(z)$$

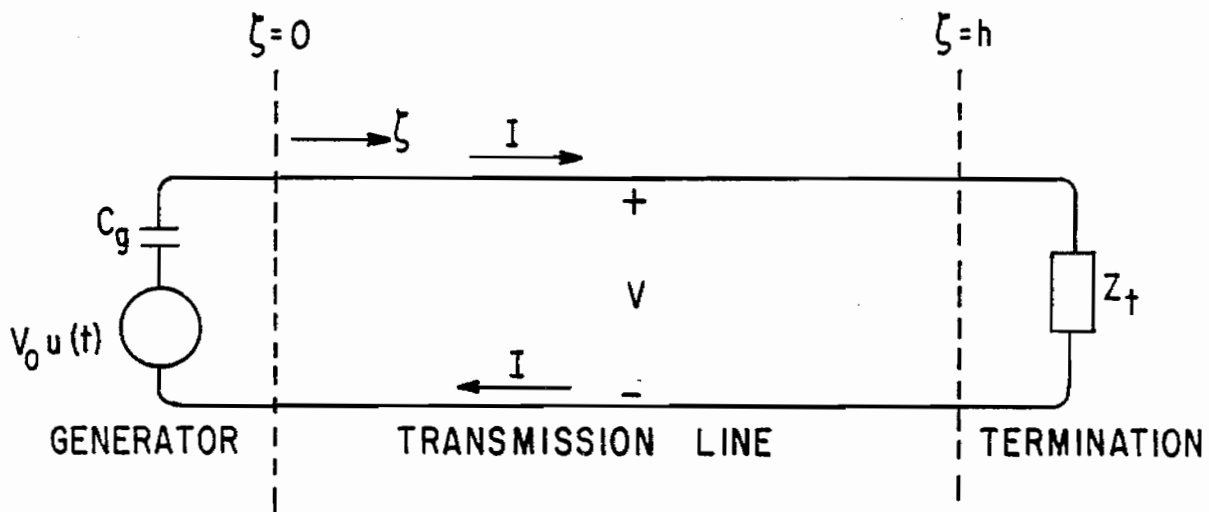
we have ζ as the coordinate, Z_t as the termination impedance, and Z' as the impedance per unit length added to the transmission line. The equivalent transmission line is formed by considering the two halves of the simulator ($z > 0$ and $z < 0$) in series, together with the constraint that Λ be even in z . The current $I(\zeta)$ is on both sides of the line with opposite directions, and $V(\zeta)$ is the voltage on the line (between opposite sides).

For the present calculations we take the generator as charged capacitor and switch which we represent as a capacitance C_g in series with a voltage source $V_{0u}(t)$ in the time domain or V_0/s in the Laplace transform domain. For the time varying voltages, currents, fields, etc. we use a tilde \sim to indicate the Laplace transform (one or two sided) of the quantity with respect to time and s for the Laplace transform variable. The inductance and capacitance per unit length are

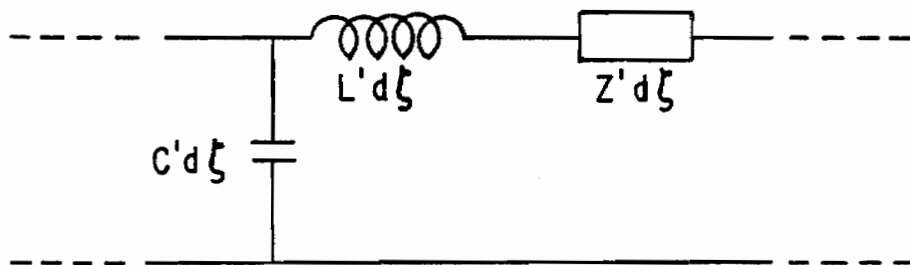
$$L' = \mu_0 f_g$$

$$C' = \frac{\epsilon_0}{f_g} \tag{71}$$

where f_g is given in equations 26 and 27 and where μ_0 and ϵ_0 are the permeability and permittivity, respectively, of free space. The speed of light is



A. TRANSMISSION LINE WITH GENERATOR



B. INCREMENTAL SECTION OF TRANSMISSION LINE

FIGURE 3. TRANSMISSION-LINE MODEL OF SIMULATOR

$$c \equiv \frac{1}{\sqrt{\mu_0 \epsilon_0}} = \frac{1}{\sqrt{L'C'}} \quad (72)$$

and the characteristic impedance of the transmission line, without including Z' , is just

$$Z_\infty = Z_0 f_g = \sqrt{\frac{L'}{C'}} \quad (73)$$

which is the same as in equation 25. Note an incremental section of the transmission line in figure 3B including L' , C' , and Z' .

The local propagation constant on the transmission line is

$$\gamma = [(sL' + Z')sC']^{1/2} = \gamma_0 \left[1 + \frac{Z'}{sL'}\right]^{1/2} \quad (74)$$

where

$$\gamma_0 = s\sqrt{L'C'} = \frac{s}{c} \quad (75)$$

The local impedance is

$$Z = \left[\frac{sL' + Z'}{sC'}\right]^{1/2} = Z_\infty \left[1 + \frac{Z'}{sL'}\right]^{1/2} \quad (76)$$

The transmission-line equations in terms of Laplace transformed variables are

$$\frac{\partial \tilde{V}}{\partial \zeta} = -(Z' + sL')\tilde{I} \quad (77)$$

$$\frac{\partial \tilde{I}}{\partial \zeta} = -sC'\tilde{V}$$

These give a wave equation (Laplace transformed) for \tilde{I} as

$$\frac{\partial^2 \tilde{I}}{\partial \zeta^2} - sC'(Z' + sL')\tilde{I} = 0 \quad (78)$$

or

$$\frac{\partial^2 \tilde{I}}{\partial \zeta^2} - \gamma^2 \tilde{I} = 0 \quad (79)$$

Note that C' is independent of ζ to give this last result. After solving for \tilde{V} and \tilde{I} equations 26 through 35 can be used to find the Laplace transforms of the fields, with restrictions as noted previously. Taking inverse transforms gives the pulse waveforms, also with certain limitations noted previously.

A previous note⁷ considers a radiating electric dipole as an approximate transmission line of constant inductance and capacitance per unit length. In that case one needed a time derivative of a volume integral of the current to obtain the radiated fields at far distances. This implied certain features for the waveform which do not appear in the present calculations because here the observer is very close to the current. The current and voltage are found in the same ways in both cases; the fields are obtained differently. In the present case L' and C' are independent of ζ because of the fixed ratio a/b for all $|z| < h$; in the case of the radiating cylindrical dipole of say constant radius the inductance and capacitance per unit length do vary with distance and using them as constants is only an approximation. Of course for the present transmission-line model of the cylinder over a ground or water surface the results are limited to only apply for radian frequencies ω small compared to c/a , and for positions with $|z| < h$. Also positions should not be near to $z = \pm h$ for both electric and magnetic fields, or near $z = 0$ for electric fields.

In this section we consider the waveforms using the transmission-line model first for a special case of resistive $\Lambda(\zeta)$ with $Z_1 = \infty$, and second for $\Lambda = 0$ with $Z_t = Z_\infty$. Finally there is some comparison of the early-time results from the transmission-line model with the more accurate early-time results discussed in section III.

A. Unterminated Transmission Line with Special Form of Nonuniform Resistive Loading

Let

$$Z_t \equiv \infty \quad (80)$$

7. Capt Carl E. Baum, Sensor and Simulation Note 81, Resistively Loaded Radiating Dipole Based on a Transmission Line Model for the Antenna, April 1969.

and consider the special case of nonuniform resistive loading used in section IV of reference 7. This case is defined by substituting

$$\tilde{I} = \tilde{F} e^{-\gamma_0 \zeta} \quad (81)$$

into equation 78 to give

$$\frac{\partial^2 \tilde{F}}{\partial \zeta^2} - 2\gamma_0 \frac{\partial \tilde{F}}{\partial \zeta} - sC'Z'\tilde{F} = 0 \quad (82)$$

Then try a solution for \tilde{F} in the form

$$\tilde{F} = f(\zeta)\tilde{F}_0 \quad (83)$$

so that \tilde{F} is split into a function of ζ times a function of s . Equations 81 and 83 define a special form for I as an outgoing wave on the simulator. The equation for $f(\zeta)$ is

$$\frac{\partial^2 f}{\partial \zeta^2} - 2\gamma_0 \frac{\partial f}{\partial \zeta} - sC'Z'f = 0 \quad (84)$$

which can be solved for Z' to give

$$Z' = \frac{1}{sC'} \frac{1}{f} \frac{\partial^2 f}{\partial \zeta^2} - 2Z_\infty \frac{1}{f} \frac{\partial f}{\partial \zeta} \quad (85)$$

which has the form

$$Z' = \frac{1}{sC''} + R' \quad (86)$$

For this type of solution for \tilde{I} then Z' is the series combination of a resistance per unit length R' and a capacitance length product C'' .

Noting (as in reference 7) that C'' represents an infinite impedance at zero frequency which prevents the maximum charge from spreading out on the simulator and thus reduces the complete time integral of I , we choose the capacitive impedance in equations 85 and 86 as zero (or $C'' = \infty$); this implies

$$\frac{\partial^2 f}{\partial \zeta^2} = 0 \quad (87)$$

so that f is a linear function of ζ . In order to match the boundary condition that $\tilde{I} = 0$ at $\zeta = h$ without introducing a second solution for \tilde{I} we then set

$$f(h) = 0, \quad f(0) = 1 \quad (88)$$

The second condition is just to normalize $f(\zeta)$. This gives

$$f(\zeta) = 1 - \frac{\zeta}{h} \quad (89)$$

From equations 85 and 70 we then have

$$Z'(\zeta) = R'(\zeta) = \frac{2Z_\infty}{h} \left[1 - \frac{\zeta}{h}\right]^{-1} \quad (90)$$

$$\Lambda(z) = \frac{R'(\zeta)}{2} = \frac{Z_\infty}{h} \left[1 - \frac{|z|}{h}\right]^{-1}$$

This specifies $\Lambda(z)$ as a resistance per unit length which has a certain z dependence and is proportional to Z_∞ which can be found from equations 25 and 26.

With this special form of $\Lambda(z)$ the transmission-line model gives a current

$$\tilde{I}(\zeta) = \left[1 - \frac{\zeta}{h}\right] e^{-\gamma_0 \zeta} \tilde{I}(0) \quad (91)$$

and a voltage (from equations 77)

$$\tilde{V}(\zeta) = \frac{1}{sC_a h} \left[\gamma_0 h \left(1 - \frac{\zeta}{h}\right) + 1 \right] e^{-\gamma_0 \zeta} \tilde{I}(0) \quad (92)$$

The simulator impedance as seen by the generator is then

$$Z_a = \frac{\tilde{V}(0)}{\tilde{I}(0)} = \frac{1}{sC_a} [\gamma_0 h + 1] = Z_\infty + \frac{1}{sC_a} \quad (93)$$

where C_a is just $C'h$ as in equation 40. Note that Z_a is just the series combination of a resistance and a capacitance. The generator impedance is just

$$Z_g = \frac{1}{sC_g} \quad (94)$$

$\tilde{I}(0)$ is then

$$\begin{aligned} \tilde{I}(0) &= \frac{V_o}{s} [Z_g + Z_a]^{-1} = \frac{V_o}{s} \left[\frac{1}{sC_g} + \frac{1}{sC_a} + Z_\infty \right]^{-1} \\ &= \frac{V_o}{s} \left[\frac{\alpha}{sC_a} + Z_\infty \right]^{-1} = \frac{V_o}{Z_\infty} \left[s + \frac{\alpha c}{h} \right]^{-1} \end{aligned} \quad (95)$$

The current on the transmission line is now

$$\tilde{I}(z) = \frac{V_o}{Z} \left[s + \frac{\alpha c}{h} \right]^{-1} \left[1 - \frac{|z|}{h} \right] e^{-\frac{s|z|}{c}} \quad (96)$$

and the voltage is

$$\begin{aligned} \tilde{V}(z) &= V_o \frac{|z|}{z} \frac{1}{s} \frac{s \left(1 - \frac{|z|}{h} \right) + \frac{c}{h}}{s + \frac{\alpha c}{h}} e^{-\frac{s|z|}{c}} \\ &= V_o \frac{|z|}{z} \left\{ \frac{1}{s} \left(1 - \frac{|z|}{h} \right) + \frac{1}{s} \frac{\frac{c}{h} \left[1 - \alpha \left(1 - \frac{|z|}{h} \right) \right]}{s + \frac{\alpha c}{h}} \right\} e^{-\frac{s|z|}{c}} \end{aligned} \quad (97)$$

Note for $s \rightarrow 0$ (low frequencies) we have

$$\tilde{I}(z) = \frac{V_o}{Z_\infty} \frac{h}{\alpha c} \left[1 - \frac{|z|}{h} \right] + O(s) = V_o \frac{C_a C_g}{C_a + C_g} \left[1 - \frac{|z|}{h} \right] + O(s) \quad (98)$$

which agrees with the previous result for an unterminated simulator in equations 45 and 46. Also for $s \rightarrow 0$ we have

$$\tilde{V}(z) = V_0 \frac{|z|}{z} \frac{1}{\alpha s} [1 + o(s)] = V_0 \frac{|z|}{z} \frac{1}{s} \frac{C_g}{C_a + C_g} [1 + o(s)] \quad (99)$$

which agrees with the previous result for an unterminated simulator in equation 42. Setting $s = i\omega$ we have the frequency content of the current and voltage waveforms. Using dimensional factors these can be converted to the frequency content of the fields using equations 26 through 35.

Now go on to consider the time-domain waveforms. Define a normalized retarded time as

$$\tau_h \equiv \frac{ct - |z|}{h} \quad (100)$$

The current is then

$$I(z) = \frac{V_0}{Z_\infty} \left[1 - \frac{|z|}{h}\right] e^{-\alpha \tau_h} u(\tau_h) \quad (101)$$

and the voltage is

$$\begin{aligned} V(z) &= V_0 \frac{|z|}{z} \left\{ \left(1 - \frac{|z|}{h}\right) + \frac{1}{\alpha} \left[1 - \alpha \left(1 - \frac{|z|}{h}\right)\right] \left[1 - e^{-\alpha \tau_h}\right] \right\} u(\tau_h) \\ &= \frac{V_0}{\alpha} \frac{|z|}{z} \left\{ 1 + \left[\alpha \left(1 - \frac{|z|}{h}\right) - 1 \right] e^{-\alpha \tau_h} \right\} u(\tau_h) \end{aligned} \quad (102)$$

These have initial discontinuities given by

$$\lim_{\tau_h \rightarrow 0^+} I(z) = \frac{V_0}{Z_\infty} \left[1 - \frac{|z|}{h}\right] \quad (103)$$

$$\lim_{\tau_h \rightarrow 0^+} V(z) = V_0 \frac{|z|}{z} \left[1 - \frac{|z|}{h}\right]$$

showing that the transmission-line model with the present particular choice of $\Lambda(z)$ gives an initial step discontinuity with a magnitude for V and I (and thus also for the fields) which falls off linearly with $|z|$, going to zero for $z = \pm h$. Of course the transmission-line model is not accurate for frequencies too large and this imposes limitations on the results of equations 103 which should be regarded as giving the early-time characteristics of the transmission-line solutions. At late time I and V become

$$\lim_{\tau_h \rightarrow \infty} I(z) = 0 \tag{104}$$

$$\lim_{\tau_h \rightarrow \infty} V(z) = \frac{V_0}{\alpha}$$

which agree with the low-frequency results of equations 98 and 99.

Equations 101 and 102 give a step rise followed by an exponential approach to the final value of the waveform with time constant $h/(c\alpha)$. In the case of the current (or magnetic field) the waveform is a simple exponential decay after a step rise, a rather convenient result. Using the results of equations 100 through 104 for I and V together with equations 25 through 35 for relating the fields to I and V gives the time-domain waveforms for the fields in terms of the various simulator parameters. Of course, note that the early-time results for times of the order of a/c and less are not accurate.

B. Terminated Transmission Line with no Resistive Loading

As another interesting case let

$$\Lambda(z) \equiv 0, \quad Z'(\zeta) \equiv 0 \tag{105}$$

$$Z_1 \equiv \frac{Z_\infty}{2}, \quad Z_t = Z_\infty$$

This defines zero resistive loading along the transmission line and a termination of the transmission line in its characteristic impedance. The simulator impedance as seen by the generator is then

$$z_a \equiv \frac{\tilde{V}(0)}{\tilde{I}(0)} = z_\infty \quad (106)$$

The current and voltage have the forms, in terms of Laplace transforms

$$\tilde{I}(z) = \frac{V_o}{z_\infty} \frac{1}{s + \beta} e^{-\frac{s|z|}{c}} \quad (107)$$

$$\tilde{V}(z) = V_o \frac{|z|}{z} \frac{1}{s + \beta} e^{-\frac{s|z|}{c}}$$

where $|z|/z$ is included to allow for the change of the electric field polarity at $z = 0$ and where

$$\beta \equiv \frac{1}{z_\infty C_g} \quad (108)$$

This result is simply a resistive-capacitive decay together with a delay for propagation down the transmission line away from the generator. Now for $s \rightarrow 0$ (low frequencies) we have

$$\tilde{I}(z) = \frac{V_o}{\beta z_\infty} [1 + O(s)] = V_o C_g [1 + O(s)] \quad (109)$$

$$\tilde{V}(z) = \frac{V_o}{\beta} \frac{|z|}{z} [1 + O(s)] = V_o C_g z_\infty \frac{|z|}{z} [1 + O(s)]$$

which agree with the results of equations 55 and 58 provided $2R_1$ is taken equal to z_∞ . Again setting $s = i\omega$ in equations 107 gives the frequency content of the current and voltage waveforms. Also using equations 25 through 35 one can convert these results to results for the fields.

Define a normalized retarded time for this case as

$$\tau_g \equiv \beta \left[t - \frac{|z|}{c} \right] \quad (110)$$

$$= \frac{1}{z_\infty C_g} \left[t - \frac{|z|}{c} \right]$$

In the time domain the current and voltage are

$$I(z) = \frac{V_0}{Z_\infty} e^{-\tau_g} u(\tau_g) \quad (111)$$

$$V(z) = V_0 \frac{|z|}{z} e^{-\tau_g} u(\tau_g)$$

These have initial discontinuities given by

$$\lim_{\tau_g \rightarrow 0^+} I(z) = \frac{V_0}{Z_\infty} \quad (112)$$

$$\lim_{\tau_g \rightarrow 0^+} V(z) = V_0 \frac{|z|}{z}$$

Note that this initial discontinuity does not decrease in magnitude with increasing $|z|$. For late times both current and voltage go to zero in agreement with the low-frequency results in equations 109.

Note for this case of a terminated transmission line without series resistive loading that both current and voltage are conveniently step rises followed by simple exponential decays to zero. Equations 111 together with equations 25 through 35 give the time-domain waveforms for the fields. Again the early-time results for times of the order of a/c and less are not accurate. Note that the half length h of the simulator structure does not enter into these results, except insofar as h must be large enough for the results to be accurate.

C. Comparison of Early-Time Results from Transmission-Line Model to More Accurate Early-Time Results

The transmission-line model gives the early-time results in equations 103 and 112 for the two cases of impedance distribution discussed in sections V A and V B respectively, when equations 25 through 35 are used to find the fields. Consider here the early time results from equations 17 in section III which give the incident-waveform peak on the $y = 0$ plane as

$$\vec{E}_{1n} \Big|_{y=0} = -za [x^2+a^2+z^2]^{-1/2} [x^2+a^2]^{-1} V_1 \vec{e}_y$$

(113)

$$\vec{H}_{1p} \Big|_{y=0} = a [x^2+a^2]^{-1} \frac{V_1}{Z_0} \vec{e}_x$$

where these are the electric field normal to the $y = 0$ plane and the magnetic field parallel to the $y = 0$ plane. Since we are considering the case of infinitely large conductivity for the lower medium then we have unity reflection coefficients for the initial peak fields and we define the resultant field components on the $y = 0$ plane, corresponding to the initial peak fields in equations 113, as

$$\begin{aligned} \vec{E}_0 &\equiv 2\vec{E}_{1n} \Big|_{y=0} \\ &= -2za [x^2+a^2+z^2]^{-1/2} [x^2+a^2]^{-1} V_1 \vec{e}_y \end{aligned}$$

(114)

$$\begin{aligned} \vec{H}_0 &\equiv 2\vec{H}_{1p} \Big|_{y=0} \\ &= 2a [x^2+a^2]^{-1} \frac{V_1}{Z_0} \vec{e}_x \end{aligned}$$

Note that, as discussed in section III, the early-time results are based on considering the pulse generator and nearby portions of the simulator structure as a radiating antenna. Since a bicone-like wave has been assumed to get the above results then only small z can be used in the above expressions, where such results are accurate if the rise time is small enough. For convenience we will then make a comparison with the transmission-line results at $z = 0$ where equations 114 reduce to

$$\vec{E}_0 \Big|_{z=0} = \vec{0}$$

(115)

$$\vec{H}_0 \Big|_{z=0} = 2a [x^2+a^2]^{-1} \frac{V_1}{Z_0} \vec{e}_x$$

Now consider the early-time transmission-line results on the $y = 0$ plane at $z = 0$. First at $z = 0$ the results of equations 103 and 112 become the same giving

$$\lim_{\tau_h \rightarrow 0^+} I(0) = \frac{V_0}{Z_\infty} \quad (116)$$

The voltage $V(z)$ is indeterminate at $z = 0$; this is associated with the limitations in the transmission-line model for calculating the electric field near $z = 0$. Clearly by symmetry the y component of the electric field is zero for all times at $z = 0$. Thus we concentrate on the magnetic field. From equations 35 and 116 the initial magnetic field at $z = 0$ on the $y = 0$ plane from the transmission-line model is

$$\begin{aligned} \vec{H}_{t_0} \Big|_{z=0} &= \frac{1}{\pi} [a^2 - b^2]^{-1/2} \frac{a^2}{x^2 + a^2} \left\{ \lim_{\tau_h \rightarrow 0^+} I(0) \right\} \vec{e}_x \\ &= \frac{V_0}{Z_\infty} \frac{1}{\pi} [a^2 - b^2]^{-1/2} \frac{a^2}{x^2 + a^2} \vec{e}_x \end{aligned} \quad (117)$$

Note that this magnetic field from the transmission-line model has the same x dependence as the radiating antenna results in equation 115 for the initial peak magnetic field.

One possible choice in designing such a simulator might be to try to match the initial peak magnetic field on $(y, z) = (0, 0)$ in amplitude as given by the two results in equations 115 and 117. Matching the two results this way implies

$$\begin{aligned} \frac{V_1}{V_0} &= \frac{Z_0}{Z_\infty} \frac{a}{2\pi} [a^2 - b^2]^{-1/2} \\ &= \frac{a}{2\pi f_g} [a^2 - b^2]^{-1/2} \end{aligned} \quad (118)$$

and as $b/a \rightarrow 0$ this becomes

$$\frac{V_1}{V_0} = \frac{1}{2\pi f_g} + o\left(\left(\frac{b}{a}\right)^2\right) \quad (119)$$

Substituting for f_g from equation 26 and V_1/V_0 from equation 8 gives

$$\begin{aligned} \ln \left[\cot \left(\frac{\theta_0}{2} \right) \right] &= \operatorname{arccosh} \left(\frac{a}{b} \right) \left[1 - \left(\frac{b}{a} \right)^2 \right]^{1/2} \\ &= \ln \left[\frac{a}{b} + \left(\left(\frac{a}{b} \right)^2 - 1 \right)^{1/2} \right] \left[1 - \left(\frac{b}{a} \right)^2 \right]^{1/2} \end{aligned} \quad (120)$$

As $b/a \rightarrow 0$ this becomes, using equations 27 and 120,

$$\begin{aligned} \ln \left[\cot \left(\frac{\theta_0}{2} \right) \right] &= \ln \left(2 \frac{a}{b} \right) + o \left(\left(\frac{b}{a} \right)^2 \right) \\ \cot \left(\frac{\theta_0}{2} \right) &= \frac{2a}{b} \left[1 + o \left(\left(\frac{b}{a} \right)^2 \right) \right] \\ \theta_0 &= 2 \operatorname{arccot} \left[\frac{2a}{b} + o \left(\frac{b}{a} \right) \right] \\ \theta_0 &= \frac{b}{a} + o \left(\left(\frac{b}{a} \right)^3 \right) \end{aligned} \quad (121)$$

This implies small θ_0 for small b/a .

An alternate approach to matching the early-time results for the radiating generator and antenna to the transmission line results would be to match the corresponding impedances. From reference 2 the pulse impedance of a bicone (as used in section III) is

$$Z_b = \frac{Z_0}{\pi} \ln \left[\cot \left(\frac{\theta_0}{2} \right) \right] = \frac{Z_0}{2\pi} \frac{V_0}{V_1} \quad (122)$$

Setting this equal to Z_∞ gives

$$\frac{1}{\pi} \ln \left[\cot \left(\frac{\theta_0}{2} \right) \right] = f_g \quad (123)$$

which with equation 26 gives

$$\ln \left[\cot \left(\frac{\theta_0}{2} \right) \right] = \ln \left[\frac{a}{b} + \left(\left(\frac{a}{b} \right)^2 - 1 \right)^{1/2} \right]$$

$$\frac{1}{\sin(\theta_0)} + \left(\frac{1}{(\sin(\theta_0))^2} - 1 \right)^{1/2} = \frac{a}{b} + \left(\left(\frac{a}{b} \right)^2 - 1 \right)^{1/2} \quad (124)$$

where we have used a trigonometric identity.⁸ Then we have as $b/a \rightarrow 0$

$$\theta_0 = \arcsin\left(\frac{b}{a}\right) = \frac{b}{a} + o\left(\left(\frac{b}{a}\right)^3\right) \quad (125)$$

For small b/a equation 123 gives nearly the same result as equation 120, so that matching early-time fields on $(x, y) = (0, 0)$ and matching impedances give approximately the same results for small b/a .

As we have seen, matching peak fields or impedances between the more accurate early-time results and the transmission-line results requires that θ_0 be a small angle for small b/a ; θ_0 is that angle defining the biconic section containing the generator, or the angle defining an equivalent distributed source with a bicone electric field distribution. However, making θ_0 small (or Z_b large) makes V_1/V_0 small and thus decreases E_1 (the peak radiated field) for a given V_0 (generator voltage). Thus one may not want to match the generator to the simulator structure in a manner given by equation 120 or 123 as discussed in this section. The early-time fields then might not smoothly match to the exponential decay as in equations 101 and 111. Of course such matching may not be the most important consideration and one may be more concerned with just the high-frequency or early-time performance (section III) and the low-frequency performance (section IV). Note also that the present comparison is made using a bicone-type wave launcher for the early-time peak fields. One may wish to use some other type of pulse radiator which gives some different peak field distribution as a function of θ and/or ϕ ; this might be achieved by some special antenna shaping or a special source field distribution on a distributed source.

8. M. Abramowitz and I. A. Stegun, ed., Handbook of Mathematical Functions, AMS 55, National Bureau of Standards, 1964, eqn. 4.3.22.

One should note that since the transmission-line results of this section are for the resultant fields they do not compare directly to the incident wave. For an infinite conductivity of the lower medium the resultant fields need to be twice the appropriate components (vertical \vec{E} and horizontal \vec{H}) of the assumed incident plane wave being simulated. Of course the lower medium actually has finite conductivity making the reflection characteristics at the $y = 0$ plane frequency dependent so that the resultant fields on the $y = 0$ plane will not in general have the same waveform as the incident wave. For the simulator then the matching of early-time results to the rest of the waveform may not be best met by the simple resulting exponential waveform in this section. The ratio V_1/V_0 may be somewhat different for an "optimum" match in such a case.

VI. Summary

In this note we have discussed various features of a simulator consisting of a pulse generator driving a cylindrical structure above and parallel to a ground or water surface. Here we have been concerned with the fields produced near the ground surface and how they simulate an incident plane wave. The considerations have included matching the early-time and low-frequency characteristics of an incident pulse plane wave with a non-zero time integral out to times beyond any times of interest. Only positions near the simulator structure are considered so that the low-frequency performance can be considered from a two-dimensional calculation. Using transmission-line theory the waveforms produced by the simulator are considered for the case that a/c is small compared to the pulse width. The early-time results from the transmission-line calculation are then compared with the more accurate early-time results based on the generator and nearby simulator structure being a radiating antenna.

In general we have seen that it is quite possible to simulate the early-time and low-frequency characteristics of an incident plane wave if the simulator is resistively terminated to the ground or water surface. Even if it is not so terminated the inclusion of series resistive loading can still give a smooth resulting waveform, except in this case if the magnetic field has a non-zero complete time integral then the electric field has a non-zero late-time limit which implies a frequency content which blows up as the frequency goes to zero. An alternate way to use such a simulator is to replace the generator by a switch and charge the two halves of the simulator with respect to each other, the transient being initiated by switch closure. For the transient waveform one can just consider $C_g = \infty$ and V_0 as the negative of the charging voltage for the present results to apply so long as the charging network is isolated from the simulator by a sufficiently large impedance and the charging is done smoothly over a time much larger than characteristic times of

interest for the transient waveform. However one should be careful to avoid any nonlinear effects in coupling to the system under test which could make the charging significant in the system response because of the large low-frequency electric field. Similar comments apply to the case of an unterminated simulator with large electric fields at late times of interest and beyond.

For a thorough understanding of this simulator geometry and the variations achievable in the waveform and frequency content there are many problems yet to be considered. Perhaps more complete wave solutions of the geometry of a perfectly conducting cylinder (or perhaps even a finitely conducting cylinder) over a finitely conducting dielectric half space could be worked out. Using such a modal expansion, or even just the dominant quasi-TEM mode, the effect of the ground or water conductivity of any value could be included, at least for radian frequencies ω small compared to c/a . In addition one might look at other types of geometries in the immediate vicinity of the pulse generator or switch near $z = 0$ as well as various types of distributed sources for generators, or even distributed switches for the case of the simulator geometry being charged from the ground or water surface. Various forms of $\Lambda(z)$ could be investigated as well as various forms of Z_1 which could include charging networks to see their effects in time and frequency domains.